PHYSICAL REVIEW B **67**, 174105 (2003)

Stability and clusterization of hydrogen-vacancy complexes in α-Fe: An *ab initio* study

Yoshitaka Tateyama and Takahisa Ohno
Computational Materials Science Center, National Institute for Materials Science (NIMS-CMSC), 1-2-1 Sengen, Tsukuba, Ibaraki 305-0047, Japan

(Received 20 January 2003; published 14 May 2003)

By means of *ab initio* supercell calculations based on the density-functional theory, we have investigated stability of hydrogen-monovacancy complexes (VH_n) and their binding preferences in α-Fe. We have found that VH_2 is the major complex at ambient condition of hydrogen pressure, which corrects the conventional model implying the VH_6 predominance. It is also demonstrated that monovacancies are not hindered from binding by the hydrogen trapping in the case of VH_2 predominance. Besides, the presence of hydrogen is found to facilitate formations of line-shaped and tabular vacancy clusters without the improbable accumulation. These anisotropic clusters can be closely associated with the fracture planes observed in experiments on hydrogen embrittlement in Fe-rich structural materials such as steel. The present results should suggest implications of hydrogen-enhanced vacancy activities to microscopic mechanism of hydrogen embrittlement in those materials.

DOI: 10.1103/PhysRevB.67.174105 PACS number(s): 61.72.Bb, 61.72.Ji, 71.15.Ap

I. INTRODUCTION

Hydrogen effects on vacancy properties in metals attract considerable attention in various points of view. Fundamentally, several new phenomena have been recently observed under hydrogen-rich conditions.[1–4] Large volume contraction under high hydrogen pressure was found in some metals including α-Fe.[1,2] This universal phenomenon was explained by an idea of superabundant vacancy formation induced by hydrogen. Enhancement of interdiffusion at the junction of two metals[3] was attributed to the difference of the hydrogen-enhanced stabilization of vacancy crucial for the diffusion process. A superlattice of hydrogen-vacancy complexes ($\mathrm{V}_m\mathrm{H}_n$) was observed in the x-ray analysis.[4] Nevertheless, the underlying interactions between solute hydrogen and vacancy in metals have not been fully understood yet.

In technological viewpoints, vacancy contributions to hydrogen embrittlement, hydrogen-induced degradation of mechanical properties, have been an interesting issue especially in Fe-rich materials such as steel.[5] Tensile experiments with hydrogen charging showed that the susceptibility of steel to hydrogen embrittlement increases with the amount of strong trap sites for solute hydrogen.[6] It was then suggested that those sites correspond to some point defects like vacancies.[7] However, no clear (quantitative) characterization has been provided on the defect states and their interactions with hydrogen. Therefore, the effects of vacancy-related processes have been still argued in spite of the plausibility.

The presence of some widely accepted models[8] also seems to prevent extensive discussion on the vacancy contributions. As the universal models for hydrogen embrittlement, lattice decohesion,[9,10] hydrogen-enhanced localized plasticity[11–14] (HELP) and so on were already evolved. These models essentially rely on the elastic effect of interstitial hydrogen, universal for various materials.[8] Consequently, they tend to be applied to a lot of materials without examination of the hydrogen concentration. Yet, their application to materials highly endothermic for hydrogen is still a matter of discussion.

In this context, establishment of quantitative understanding of hydrogen-vacancy interactions in α-Fe is quite indispensable for further discussion of the microscopic mechanism of hydrogen embrittlement in those Fe-rich materials. The knowledge obtained in such investigations will be of great use for control of material properties by changing hydrogen condition.

The nature of hydrogen-vacancy complexes in α-Fe, in fact, was extensively examined in terms of plasma-wall interaction in fusion reactors, not hydrogen embrittlement, over a decade ago. Implantation-annealing experiments have revealed some hydrogen trapping energies of vacancies.[15,16] Then, a model on multiple trapping of hydrogen in a monovacancy[16,17] was proposed in conjunction with the results of the effective-medium theory[18] (EMT) calculations. This model has been referred as a settled one to date.[2,19] However, we should point out that the model itself still involves several inconsistencies.

In general, there are six sites possible to trap hydrogen in a monovacancy of a bcc metal. They are located near octahedral *O* sites adjacent to the vacancy[20] as shown in Fig. 1. The experiments imply two characteristic states on the hydrogen trapping of monovacancy in α-Fe. The energies trapping a hydrogen atom from an interstitial site were estimated to be 0.63 and 0.43 eV with the help of a transport model.[16]

The EMT calculations, on the other hand, gave the result that the hydrogen trapping energies for the VH and VH_2 formations are about 0.8 eV, while those of VH_3–VH_6 are estimated between 0.45 and 0.55 eV.[16,17] From these results, it was concluded that the experimental 0.63-eV state corresponds to hydrogen trapping for VH and VH_2, while the 0.43-eV state for VH_3–VH_6.[16,17] Since the heat of solution for interstitial hydrogen in α-Fe is 0.29 eV,[21] this conclusion implies that all of the six sites in the monovacancy are exothermic for hydrogen. Namely, hydrogen in the VH_6 complex is energetically favorable than that in the H_2 molecule in vacuum. Thus VH_6 is regarded as the most major complex at ambient condition of hydrogen pressure.[2,17,19]

However, one can see a distinct difference in the absolute

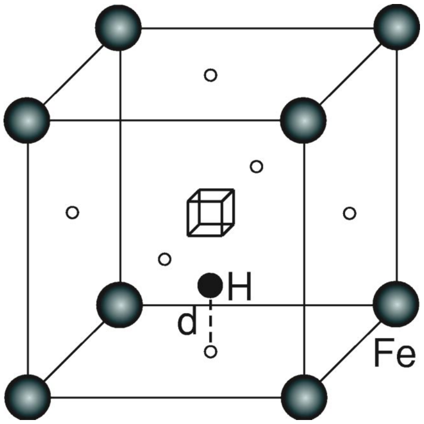

FIG. 1. Schematic view of a hydrogen-monovacancy complex VH_1 in bcc α-Fe. The transparent cube at the body center expresses the monovacancy. Gray spheres show Fe atoms and the black one is hydrogen. Six open circles located at the face centers of the cubic lattice are octahedral *O* sites. Each hydrogen atom is located near the corresponding *O* site. The distance between them is referred as *d* throughout this paper.

values of hydrogen trapping energies between the experiment and the EMT calculations. Besides, the deduced model implies significant decrease of the monovacancy formation energy in α-Fe by trapping six hydrogen atoms. The decrease corresponds to the sum of heats of solution for $VH-VH_6$ formations, which is estimated to be 1.43 eV according to the above assignments.[17] Since the experimental monovacancy formation energy is about 1.6–2.0 eV,[22,23] this energy decrease leads to a serious increase of vacancy concentration even at ambient pressure of hydrogen gas and room temperature, whereas such extreme vacancy formation has not been reported at the condition as yet.

The model of the VH_6 predominance at ambient condition will also affect the binding properties of vacancies. Concerning divacancies in α-Fe, it was reported from the empirical potential analysis that $\langle 100\rangle$ divacancy [Fig. 2(a)], a monovacancy occupying a second nearest-neighbor site of the other, is energetically most favorable.[24] With respect to the VH_6 binding, it is naively expected that the $\langle 100\rangle$ divacancy reduces the number of hydrogen trap sites and forces an excess hydrogen atom to go out of the vacancy and occupy an interstitial site. This is likely to increase the total energy of the system, which makes the vacancy binding energetically unfavorable in the presence of hydrogen. Thus the stability of VH_n largely affects the binding preference and finally the defect behaviors in the materials.

In order to elucidate the nature of hydrogen-vacancy complexes in α-Fe, thus, more precise examinations should be still indispensable. However, experimental approaches to solute hydrogen in α-Fe are quite limited owing to the extremely low solubility of hydrogen. In this context, computational approach with accuracy would be a most promising tool to address the problem.

In this paper, we investigate the stability and binding properties of VH_n in α-Fe by means of *ab initio* calculations based on the density-functional theory (DFT).[25,26] Zero-point motion energy of hydrogen, which is also important in the study of hydrogen, is evaluated by Schrödinger equation with adiabatic potential. The results provide a different insight into the fundamental nature of VH_n complexes in α-Fe, which can explain various experimental results in contrast to the previous calculations.[16,17] We then examine the energetics of vacancy clusters beyond divacancy in the presence of hydrogen in α-Fe. Finally, we discuss the relevance of vacancy-related processes to hydrogen embrittlement in Fe-rich materials from a microscopic viewpoint.

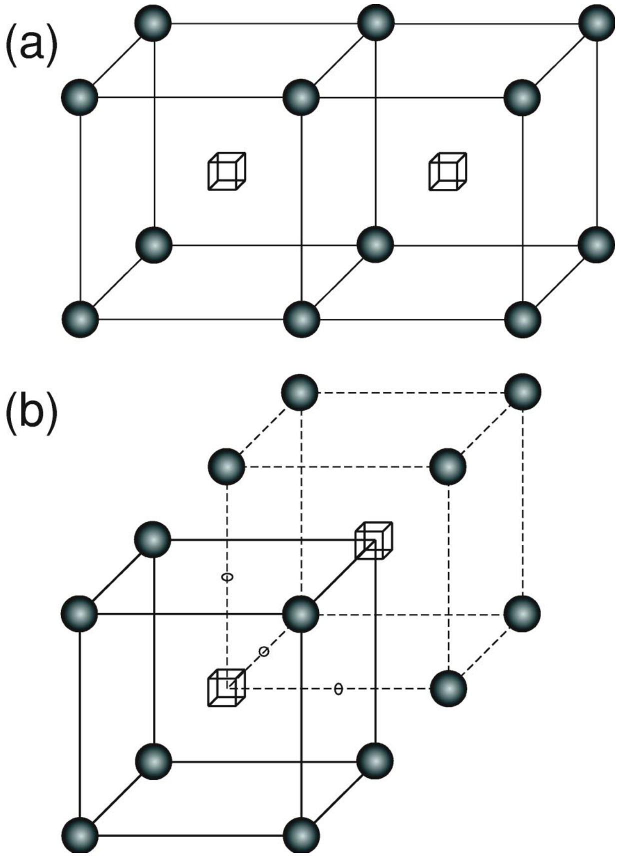

FIG. 2. Schematic views of (a) $\langle 100\rangle$ and (b) $\langle 111\rangle$ divacancies.

This paper is organized as follows: In Sec. II, we first describe the method and conditions we have used in the calculations. Some detailed formulations of the energetics of hydrogen-vacancy complexes are also presented. In Sec. III, we examine vacancies without hydrogen in α-Fe, mainly to demonstrate the accuracy of our calculations. We then investigate the stability of hydrogen-monovacancy complexes and their binding preferences in α-Fe. Application of the vacancy-related processes to the hydrogen embrittlement mechanism in Fe-rich materials is also discussed. A summary of the present findings is presented in Sec. IV.

II. CALCULATION DETAILS

Our electronic state calculations are based on DFT.[25,26] Compared to EMT used in the previous calculations, DFT can equivalently deal with various chemical states such as covalent, ionic, as well as metallic bonds. Among several types of DFT-based *ab initio* calculation methods, we use a

TABLE I. Lattice constant a_0 (Å), bulk modulus B_0 (GPa), and magnetic moment M_0 (μ_B per atom) of pure α-Fe obtained in our *ab initio* calculations with the results of other calculations and experiments (Ref. 33) Calculated heat of solution for interstitial (solute) hydrogen E_s (eV/H) is also compared with the experimental values.

	Our calculations	Other calculations	Expt.
a_0 (Å)	2.85	2.86,[a] 2.76[b]	2.86
B_0 (GPa)	152	155,[a] 235[b]	168
μ_0 (μ_B per atom)	2.24	2.32,[a] 2.05[b]	2.22
E_s (eV/H)	0.34		0.29[c]

[a] Reference 34; GGA results.

[b] Reference 34; LDA results.

[c] Reference 21.

method employing plane-wave basis set along with pseudopotential technique.[27] This method has an advantage that relaxed atomic configurations as well as electronic states can be easily and accurately calculated. For defect properties in $3d$ transition metals where localized electronic states and atomic relaxations are important, the method we employed is most suitable.

In this study, we use the *ab initio* code STATE developed by Morikawa *et al.*[28] to carry out electronic state calculations and structure optimizations. We utilize an ultrasoft pseudopotential.[29] The cutoff energies of plane-wave basis for wave functions and augmented charge are 25 and 289 Ry, respectively. A spin-polarized generalized gradient approximation[30] (GGA) is used for the exchange-correlation energy. GGA is known to be essential to obtain the bcc ferromagnetic phase as the ground state of iron at zero pressure.[31] Taking spin polarization into account is crucial for the vacancy stability in α-Fe, since the monovacancy formation energy is found to vary with the magnetic state in the previous studies.[22,32]

Most of our calculations use a supercell consisting of 54 bcc sites, aiming at accurate estimation of point defect properties. We use 27k points for integration of full Brillouin zone (FBZ) of the supercell. This is equivalent to making use of about 1500 points for FBZ of the bcc primitive cell. Preliminary calculations to fix this condition will be described below. These conditions give lattice constant (2.85 Å), bulk modulus (152 GPa), and magnetic moment (2.24 μ_B) of pure α-Fe, in good accordance with the results of experiments[33] and other accurate calculations with GGA,[34] as shown in Table I.

Energies of hydrogen-vacancy complexes are calculated by means of formulations in the supercell scheme.[35] In this scheme, monovacancy formation energy is formulated as

$$E_{1V}^{F}=e(1,0,V)-\frac{N-1}{N}e(0,0,V_0). \tag{1}$$

Throughout this paper, N is the number of lattice sites in the supercell, and $e(N_V,N_H,V)$ denotes the calculated energy of the supercell involving N_V vacancies and N_H hydrogen atoms at the cell volume V. The volume V_0 means the equilibrium one of the supercell for the perfect lattice. This is often expressed as $N\Omega_0$, where Ω_0 is the equilibrium atomic volume in the perfect lattice.

There are several manners to deal with the volume V of the supercell containing a monovacancy, depending on the targets to be examined. In terms of enthalpy at zero pressure, $H_{1V}^{F}(p=0)$, the relaxed volume to the given pressure should be used. In this case, the vacancy formation volume can be obtained by the following formulation:

$$\Omega_{1V}^{F}=V-(N-1)\Omega_0. \tag{2}$$

The relaxation (contraction) volume due to the monovacancy formation is expressed as $\Omega_0-\Omega_{1V}^{F}$. These quantities are inherent properties of the monovacancy, and thus should be independent of the supercell size.

If the supercell is large, the ratio of the relaxation volume to the total one becomes quite small. In this case, energy change caused by the volume relaxation due to the vacancy formation can be negligible, since the elastic energy depends on the volume ratio, not the absolute volume. Thus the constant-volume manner fixing the supercell volume to $V_0=N\Omega_0$ becomes reasonable if a large enough supercell is used. In the present conditions, the energy changes by the volume relaxations are found too small as described later, so that we primarily use the results within the constant-volume manner in the following discussion. Note that local lattice relaxations essential for defect properties are, on the other hand, carried out in all of the present calculations.

Following these formulations, we have defined the total energy of arbitrary hydrogen-vacancy complex at ambient condition of hydrogen pressure (chemical potential). The total energy of V_mH_n at the supercell volume V, $E(m,n,V)$, is expressed as

$$E(m,n,V)=e(m,n,V)-\frac{N-m}{N}e(0,0,V_0)-\frac{n}{2}e_{H2}, \tag{3}$$

where e_{H2} is the total energy of H_2 molecule in vacuum. The monovacancy formation energy E_{1V}^{F} described above corresponds to $E(1,0,V)$. This expression is easily extended to the case of finite chemical potential of H_2 molecule (μ_{H2}) as follows:

$$E(m,n,V;\mu_{H2})=E(m,n,V)-\frac{n}{2}\mu_{H2}. \tag{4}$$

The hydrogen-trapping (binding) energy for V_mH_n, which is defined as the energy gain by trapping an interstitial hydrogen atom into a vacancy site to form V_mH_n, is expressed as follows:

$$\begin{aligned}E_{trap}(m,n)=&\{E(m,n-1,V')+E(0,1,V_1)\}\\&-\{E(m,n,V)+E(0,0,V_0)\},\end{aligned} \tag{5}$$

where $E(0,1,V_1)$ denotes the total energy of the system containing one interstitial hydrogen atom. Although there are several volumes in this formulation, which leads to some complications in the calculations, negligible energy variation to the volume change clears off such difficulties.

As the interstitial hydrogen state in α-Fe, we suppose a hydrogen atom located at a tetrahedral (T) site. As is known, the ground state of interstitial hydrogen in α-Fe has been still a matter of discussion, since a delocalized state tunneling among some potential minima was suggested to be possible.[19] We have extensively examined this problem and concluded the hydrogen localized around a T site to be the ground state, which will be described elsewhere in detail.[36] Zero-point motion energy for such hydrogen at a T site has been calculated by means of the Schrödinger equation with an adiabatic potential evaluated by *ab initio* calculations. The resultant energy is 0.20 eV/H.

Heat of solution for the interstitial hydrogen state is calculated as the energy difference from that of H_2 molecule in vacuum. In conjunction with hydrogen atom energy in our *ab initio* calculations and the experimental dissociation energy of H_2 molecule,[37] we have obtained 0.32 eV/H of the heat of solution. This is in good agreement with the experimental value of 0.29 eV.[21]

Regarding zero-point motion energies for VH_n complexes, we found that those in $\mathrm{VH}_n(n=1-4)$ are very similar (0.135–0.145 eV/H). Potential curvature perpendicular to the nearby $\{100\}$ plane increases with n, while oscillation energy along the parallel directions becomes small. Based on these results, we employ 0.14 eV/H, the average so far, for zero-point motion energies of all the complexes. In practice, we add $0.14n$ to $e(m,n,V)$ in Eq. (3), which almost cancels out the zero-point motion energy of $(n/2)$ H_2 molecules (0.14 eV/H) included in the last term of Eq. (3). It is found that this approximation does not affect the conclusions.

In the exploration of binding possibility of VH_n complexes, we examine two types of divacancies, monovacancies aligned in the $\langle 100\rangle$ and in the $\langle 111\rangle$ directions. This is because it was reported that the former is the most stable and the latter is the next in the early work on vacancies in α-Fe using classical potentials.[24] Their schematic views are shown in Fig. 2.

III. RESULTS AND DISCUSSION

A. Vacancies without hydrogen

First, we have calculated vacancy properties without hydrogen in order to search optimal calculation conditions and evaluate the energy convergence. Here we calculate electronic states in metallic systems, so that dependence of energies on the k-point density in the calculation is one issue to be checked. The total energy of perfect lattice and several vacancy formation energies with respect to the effective number of k points for FBZ of the bcc primitive cell (N_k^0) are shown in Table II. The ΔE_{tot} indicates that the convergence for the perfect lattice is achieved around $N_k^0=432$. The vacancy formation energies seem to be converged in the same condition within an error of 0.1 eV, whereas the relative stability of the two divacancies is not converged yet. Thus we employ the $N_k^0=1458$ condition, namely, a 54-sites supercell with $27k$ point. These data clearly show that a more severe condition is necessary for convergence of defect-related energies than the case of perfect lattice.

TABLE II. Representative energies of α-Fe calculated in the N_s-site supercell with N_k k points. The number of k points in the bcc primitive cell corresponding to each condition is expressed as N_k^0. ΔE_{tot} (eV/atom) is total energy of perfect lattice compared to that in the 54-site supercell with $27k$ points which we mainly used in this study. The formation energies of monovacancy E_{1V}^F, $\langle 100\rangle$ divacancy $E_{2V,100}^F$, and $\langle 111\rangle$ divacancy $E_{2V,111}^F$ are also shown in eV.

N_s	N_k	N_k^0	ΔE_{tot}	E_{1V}^F	$E_{2V,100}^F$	$E_{2V,111}^F$
54	1	54	−0.108	2.37	4.56	4.37
128	1	128	0.046	1.85	3.62	3.59
54	8	432	−0.007	2.02	4.01	4.00
128	8	1024	−0.005	2.10	3.96	4.02
54	27	1458	0	2.00	3.85	3.92
54	64	3456	−0.004	2.04	3.91	3.97

Comparison with respect to the supercell size is another matter of concern. The vacancy formation energy ($V=V_0$), enthalpy at zero pressure (relaxed V), and the formation volume are listed in Table III, where the results of 54-site and 128-site supercells are shown. The difference in the absolute energies is found to be about 0.1 eV. This does not alter

TABLE III. Formation energies without volume relaxation E_X^F (eV), enthalpies for the relaxed volume at zero pressure H_X^F (eV), and formation volumes $\Omega_X^F(/\Omega_0)$ in α-Fe calculated by use of a 54-site supercell ($27k$ points) and a 128-site one ($8k$ points). Note that all the present results take local lattice relaxations into account. The results of previous *ab initio* calculations (LSGF-LDA, FPLMTO-LDA, PWPP-GGA) are also listed. Details of those calculations are described in the text. Experimental results are also shown.

X	E_X^F (eV)	H_X^F (eV)	Ω_X^F $(/\Omega_0)$
V			
54-site	2.00	2.00	0.86
128-site	2.10	2.09	0.80
LSGF-LDA[a]		2.25	0.55
FPLMTO-LDA[b]		2.76	
PWPP-GGA[c]		1.95	0.90
Expt.[d]		1.6–2.0	0.95
$V_2\langle 100\rangle$			
54-site	3.85	3.84	0.65
128-site	3.96	3.95	0.70
$V_2\langle 111\rangle$			
54-site	3.92	3.91	0.74
128-site	4.02	4.01	0.72

[a] Reference 32.
[b] Reference 38.
[c] Reference 39.
[d] References 22 and 23.

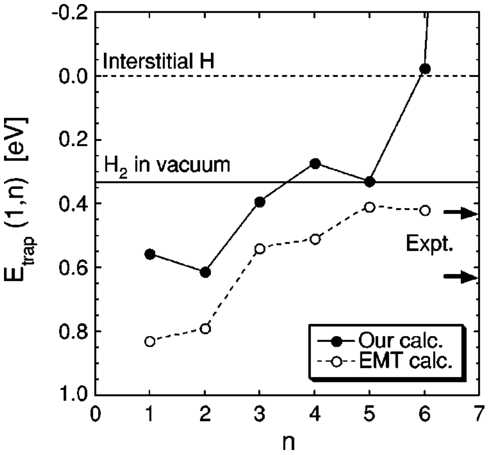

FIG. 3. Calculated hydrogen trapping energies in α-Fe (filled circles). The open circles and arrows show the results of EMT calculations and experiments, respectively. The energies at a interstitial site (origin) and in H_2 molecule in vacuum at ambient condition are shown by horizontal broken and solid lines, respectively. The H_2 energy minus the VH_n one corresponds to the heat of solution at the H trapping from vacuum into VH_{n-1} forming VH_n.

binding preference of the two monovacancies as well as relative stability between the two divacancies. Regarding the formation volume, the relative magnitude is not changed by the supercell size. Thus convergence even on the divacancy properties is achieved in the 54-site supercell with 27*k* points, which allows us to examine binding behaviors of monovacancies.

The effects of volume relaxation have also been checked. Energy reduction by the volume relaxation are found to be within 0.01 eV for both monovacancies and divacancies in the present conditions. This demonstrates that the size of a 54-site supercell is sufficiently large, and allows us to discuss the present problems with the constant-volume manner.

Finally, we make a comparison with results of other calculations and experiments. Calculations using locally self-consistent Green's function[32] (LSGF) and full-potential linear muffin-tin orbital[38] (FPLMTO) methods rather overestimate the monovacancy formation energy and underestimate the formation volume. This is mainly ascribed to their way that only volume relaxation was included. Also, local-density approximation (LDA) has some contribution. On the other hand, inclusion of local lattice relaxation and use of GGA gave much better formation energy and volume,[39] where the *ab initio* method using plane-wave basis with pseudopotentials (PWPP), equivalent to ours, is used. These again ensure that our investigation taking local lattice relaxation into account and using GGA is quite reasonable for the present targets.

B. Stability of hydrogen-monovacancy complexes

Hydrogen trapping energies for VH_n are shown in Fig. 3 with the EMT and experimental results. Note that the EMT results involve the zero-point motion effects of hydrogen as well as ours. We found that the VH_6 formation has almost zero in the trapping energy. The energies for VH and VH_2 formations are about 0.60 eV, which correspond to the 0.63-eV state in experiments. Also, the experimental 0.43-eV state is regarded as VH_3 formation, because the trapping energy is 0.40 eV in our calculations. Agreement between our trapping energies and experimental values is quite good, compared to the EMT results.[16,17]

The heat of solution for VH_n, which is the energy compared to H_2 molecule in vacuum at ambient condition, suggests that VH and VH_2 are completely exothermic for hydrogen and almost zero is VH_3. On the other hand, the VH_4 and VH_5 formations are slightly endothermic, and the sixth hydrogen in VH_6 has no energy gain at the trapping from an interstitial site. These indicate that VH_2 is the major complex at ambient condition owing to the large negative heat of solution for hydrogen, and slight increase of chemical potential of H_2 may lead to an increase of the VH_3 population. This conclusion is in good agreement with the experimental observation that the 0.63-eV state exists even at ambient condition, while the 0.43-eV state appears with increase of implanted hydrogen isotopes.[16] It is also consistent with the observation of 0.46 eV of hydrogen-trapping energy after quenching from high H pressure.[2] Hence our calculations well explain the experiments quantitatively as well as qualitatively, in contrast to the conventional model based on the EMT results. In consequence, it is demonstrated that the major complex in α-Fe at ambient condition of hydrogen chemical potential is VH_2, not VH_6 as believed to date.

Hydrogen effects on vacancy concentration (formation) are also very interesting. The formation energy of VH_n is defined as the monovacancy formation energy minus the sum of heats of solution for VH_1–VH_n. At ambient condition of hydrogen pressure, the VH_2 formation energy is 1.51 eV in our calculations. This does not lead to an unrealistic large amount of vacancy formation resulting from the conventional model as described above. We should point out that the VH_2 formation energy is lower than the monovacancy formation without hydrogen by about 0.5 eV at ambient condition. According to Boltzmann statistics at 300 K, this energy reduction leads to a 10^7 times increase of vacancy density by trapping two hydrogen atoms. Thus enhancement of vacancy formation in the presence of hydrogen is still very remarkable. This result is a clear evidence of enhancement of vacancy formation by "hydrogen trapping" suggested by Fukai and co-workers.[1,2]

What determines the stability of VH_n? We first examine the problem in terms of the electronic states of VH_n. Figure 4 shows densities of states (DOS) in the V and VH_2 complexes. The DOS of VH_2 indicates that a new state appears below the 4*s* band of pure α-Fe by trapping hydrogen atoms in monovacancy. Partial electron density of these new states clearly indicates Fe 3*d*-H1*s* hybridization as shown in Fig. 5. This hybridization is responsible for the large hydrogen trapping energies for VH_2 (and VH) formation through the termination of broken Fe bonds.

The new state has a bonding character mainly consisting of H 1*s* orbital and is doubly occupied by electrons. This indicates electron transfer to the region around the hydrogen atoms from the neighbor Fe. The resulting negatively charged hydrogen atoms repel each other. The repulsive in-

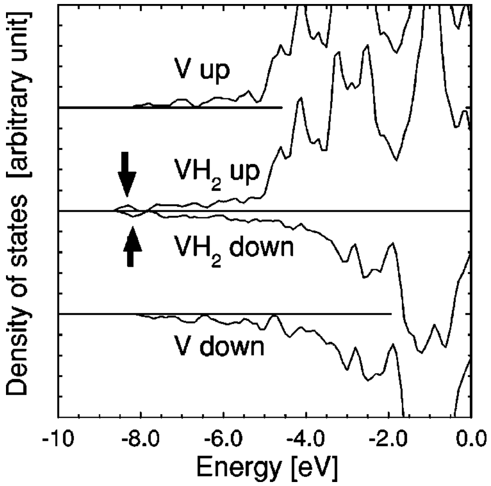

FIG. 4. Density of states for up- and down-spins in the V and VH_2 complexes in α-Fe. New states clearly appearing in the VH_2 are pointed by black arrows. The energy origin is set to the Fermi energy.

teraction seems to become more dominant with increase in the number of trapped hydrogenatoms. This can explain the abrupt decrease of hydrogen trapping energies for $VH_n(n \geqslant 3)$. Consequently, the competition between hybridization and Coulombic repulsion makes VH_2 the major complex at ambient condition. These results demonstrate that the EMT method is not adequate to the present system, because it mainly deals with hydrogen interaction with delocalized states (e.g., Fe $4s$) of electrons.[18]

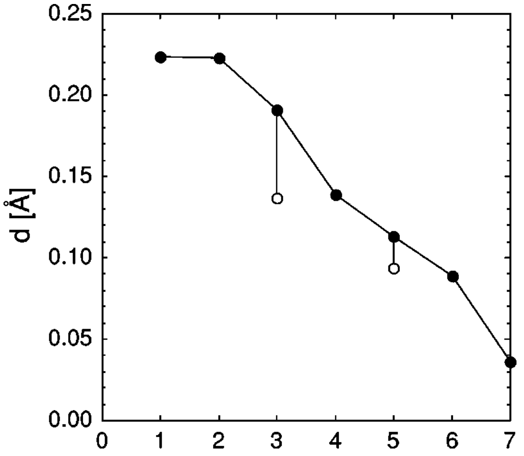

FIG. 6. Distances between hydrogen atoms and the corresponding O sites in the VH_n complexes in α-Fe. Closed and open circles show the maximum and minimum distances. Owing to the large symmetry breaking, the differences among the distances are large in the VH_3 and VH_5 complexes.

This view is supported by change of hydrogen positions depending on the number of hydrogen atoms in the monovacancy. The distances between hydrogen atoms and the corresponding O sites in each VH_n complex are shown in Fig. 6. We found that the distances do not alter between VH and VH_2, suggesting that the hybridization effect prevails in these complexes. At $n \geqslant 3$, on the other hand, the distance gradually decreases with n. This agrees with the explanation that the repulsion effect becomes effective in those complexes.

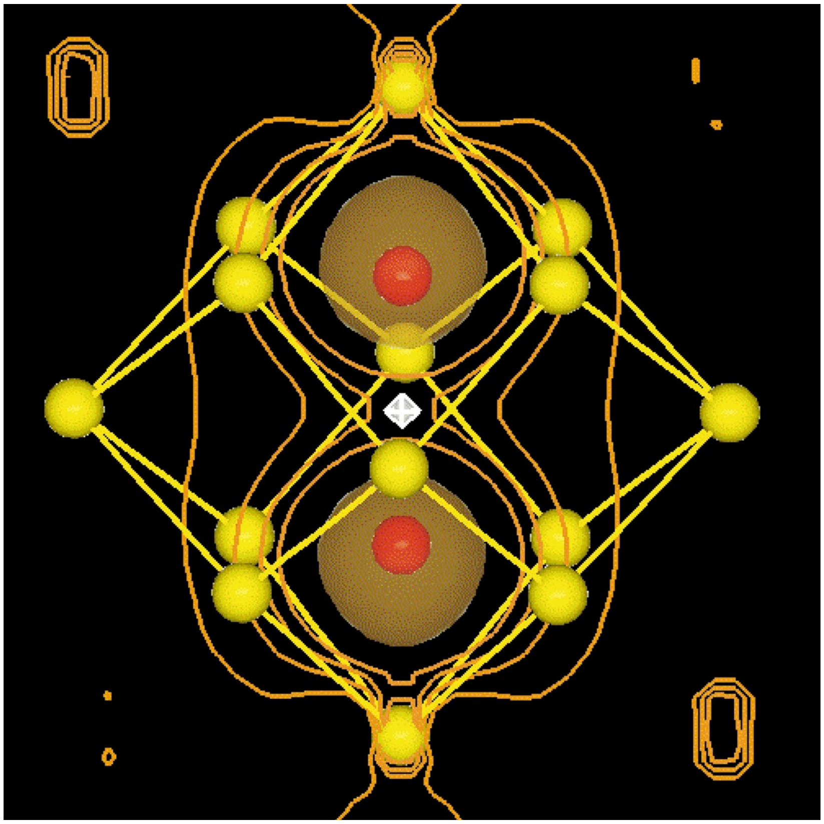

FIG. 5. (Color) Atomic configurations and partial charge densities of the minimum-energy structure of VH_2. Yellow and red spheres express Fe and H atoms, respectively, while the white diamond indicates a vacancy. For visibility, only Fe atoms and bonds surrounding the vacancy are shown. The three-dimensional (3D) isosurfaces around H show the partial charge density ($\rho = 0.004$) of the new states appearing with the H trapping. Orange 2D contours express the density ($\rho = 0 - 0.002$) on the (010) plane through the H atoms, which clearly demonstrate Fe $3d$–H $1s$ hybridization.

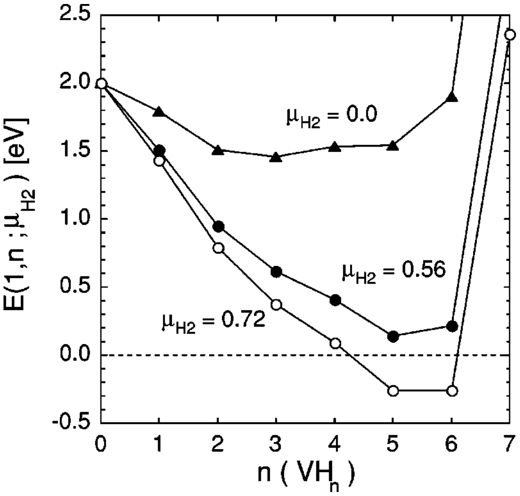

FIG. 7. Total energies of VH_n in several chemical potentials (pressures) of hydrogen gas. The potentials $\mu_{H2} = 0, 0.56$, and 0.72 eV correspond to 0, 1, and 2 GPa of H_2 pressures. Between 1 and 2 GPa, negative vacancy formation energy is realized, which is in good agreement with the experimental observation of superabundant vacancy formation at the H_2 pressure of 1.7 GPa.

When a hydrogen atom is put at the substitutional position in the examinations of VH stability, we found that the hydrogen relaxes to the equilibrium position without any barrier. We also put H_2 molecule in the vacancy. But H_2 dissociates and moves to the equilibrium positions. This suggests that if the vacancy cluster is small, H_2 molecule could not survive in the cluster. So, the previous models on hydrogen embrittlement where accumulated H_2 pressure expands the voids leading to crack initiation may be questionable in the initial stage.

Our results can be also compared with those in the experiment using high hydrogen gas pressure. According to Sugimoto and Fukai,[40] compressive H_2 pressures of 1 and 2 GPa at 500 K approximately correspond to H_2 chemical potentials μ_{H2} of 0.56 and 0.72 eV, respectively. Using these potentials, we have calculated the formation energies of VH_n at these H_2 pressures, which are shown in Fig. 7. The result clearly indicates that negative formation energy is realized between 1 and 2 GPa in H_2 pressure. This is in excellent agreement with the observation of superabundant vacancy formation in α-Fe at 1.7 GPa of H_2 pressure.[2] In such a pressure region, VH_5 and VH_6 become the major complexes.

C. Hydrogen effects on vacancy clusterization

We next investigate binding preference of VH_n complexes in α-Fe. The binding energy (energy gain at the binding) of two VH_n complexes is calculated by means of following formulation:

$$E_b = E(2,2n,V') + E(0,0,V_0) - 2E(1,n,V). \tag{6}$$

Each term in the right-hand side of the formulation is independently calculated with the corresponding relaxed volume (V or V'), in principle. However, owing to the convergence of the present supercell size as described above, we primarily use the constant-volume manner. The results are listed in Table IV.

TABLE IV. Calculated binding energies of VH_n complexes in α-Fe. Positive energy indicates that the binding is energetically favorable. The energies for the rigid as well as relaxed Fe lattices are listed, where hydrogen positions are fully relaxed in both cases. The former energy reflects the electronic (chemical) contribution to the binding, while the difference between the two energies in the same system reveals the effect of local lattice relaxation.

Reactants	Products	E_b (eV)
Relaxed Fe lattice		
2 V	$V_2\langle 100\rangle$	+0.15
2 V	$V_2\langle 111\rangle$	+0.08
2 VH_2	$V_2H_4\langle 100\rangle$	−0.06
2 VH_2	$V_2H_4\langle 111\rangle$	+0.18
2 VH_6	$V_2H_{12}\langle 100\rangle$	−2.60
2 VH_6	$V_2H_{11}\langle 100\rangle$	
	+Interstitial H	−0.57
Rigid Fe lattice		
2 V	$V_2\langle 100\rangle$	+0.21
2 V	$V_2\langle 111\rangle$	+0.19
2 VH_2	$V_2H_4\langle 100\rangle$	−0.06
2 VH_2	$V_2H_4\langle 111\rangle$	+0.27

In the case without hydrogen ($n = 0$), binding energies to the $\langle 100\rangle$ and $\langle 111\rangle$ divacancies are calculated to be +0.15 and +0.08 eV, respectively. Unfortunately, no experimental data are available for comparison. However, the same relative stability and similar energy difference for the two divacancies were obtained in the recent *ab initio* calculations with the VASP code as well.[39] Thus the preference to $\langle 100\rangle$ divacancy may be regarded as the conclusion in terms of *ab initio* GGA calculations. Note that, surprisingly, the study using classical Johnson's potential over three decades ago came to the same conclusion.[24]

As described in Sec. I, the binding of VH_6 complexes is a matter of concern. We have calculated two binding manners; one is the formation of V_2H_{12}, and V_2H_{11} (with an interstitial hydrogen atom escaping from the cluster) is the other. The results have clarified that both these processes are energetically unfavorable, as previously expected. Therefore, following the conventional model based on the VH_6 predominance at ambient condition, one might have concluded that the vacancy binding is unfavorable in the presence of hydrogen.

However, the present finding of the VH_2 predominance leads to the opposite conclusion. The $V_2H_4\langle 111\rangle$ formation by binding two VH_2 complexes is found to have a binding energy of +0.18 eV, thereby being energetically favorable (Table IV). Thus we can conclude that the vacancy binding is preferred in the presence of hydrogen at ambient condition. Furthermore, the binding energy is larger than those without hydrogen (e.g., +0.15 eV), so that the presence of hydrogen is likely to slightly facilitate (or not to suppress at least) the binding processes. The minimum-energy configuration of hy-

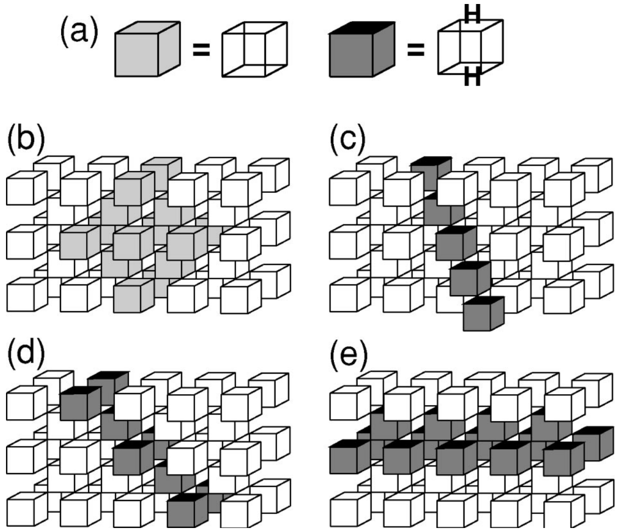

FIG. 8. Schematic view of probable vacancy cluster configurations. (a) The light gray cube denotes monovacancy without H, while the dark one indicates the directional VH_2 unit where the black plane expresses H occupation near the plane. A probable configuration without H is shown in (b). A line-shaped, a tabular {110} as well as a tabular {100} VH_2 clusters probable in the presence of hydrogen are shown in (c–e), respectively.

drogen atoms in the V_2H_4 complex shows that orientations of the hydrogen pairs in both VH_2 constituents are aligned in the same direction. This suggests that the atomic configuration of VH_2 (Fig. 5) can be a directional unit to the formation of larger V_nH_{2n} clusters [Fig. 8(a)].

Based on these results, we explore the larger cluster formations. Here we divide the binding energy of each vacancy cluster into the contributions from the electronic rearrangement and from the local lattice relaxation. The former is obtained by calculating the energy without any lattice relaxation, namely in the rigid Fe lattice. The difference between this energy and the fully-relaxed one corresponds to the local lattice relaxation effect. We show the binding energies of some clusters in the rigid lattice in Table IV as well.

Without hydrogen, electronic contributions of the binding energies are about $+0.2$ eV ($+0.19$ or $+0.21$ eV), while the local lattice relaxation effects are roughly -0.1 eV (-0.06 or -0.11 eV). Accordingly, the former positive contribution of the electronic rearrangement at the binding is found more dominant. This intrinsic preference of the binding implies that the total binding energies for V_n cluster at arbitrary n will be also positive.

We also found that the lattice relaxation effects primarily make a difference between $V_2\langle 100\rangle$ and $V_2\langle 111\rangle$. Examination of the local lattice relaxations indicates that the $V_2\langle 100\rangle$ cluster has larger relaxation around the binding region. This seems responsible for more increase of the binding energy, namely decrease of the total energy. These indicate that a cluster allowing larger lattice relaxation, namely a more compact (spherical) cluster, is energetically favorable in the case without hydrogen as shown in Fig. 8(b). The same conclusion was obtained in Ref. 24 for V_n with large n.

If the $\langle 111\rangle$ binding is predominant, formation of larger clusters of the VH_2 complexes seems likewise energetically favorable in terms of the context that the electronic contribution (involving hydrogen relaxation in this case) for the $\langle 111\rangle$ binding ($+0.27$ eV) overcomes the lattice relaxation effect. On the other hand, there is another characteristic in the clusterization of VH_2. The energy gain by Fe-H hybridization in the VH_2 formation is 0.5 eV/H_2. If a hydrogen atom in a VH_2 complex loses its site at the binding, the energy loss of 0.25 eV/H for the Fe-H bonding is expected in the binding energy. Since this energy is larger than $+0.18$ eV, the loss of hydrogen sites finally leads to the negative binding energy. As a consequence, this Fe-H hybridization is also predominant in the energetics of $(VH_2)_n$.

These considerations indicate that VH_2 complexes are likely to favor not only line clusters along the $\langle 111\rangle$ directions but also tabular ones along {110} or {100} plane as shown in Fig. 8, so as to keep the hydrogen sites as well as the $\langle 111\rangle$ binding networks. Thus we have found that the presence of hydrogen will induce anisotropic clusterizations of vacancies in α-Fe. This finding will be crucial for understanding various phenomena induced by hydrogen as well as more active applications such as control of internal defects by hydrogen.

D. Potential vacancy contributions to hydrogen embrittlement

Our present findings of the hydrogen effects on vacancy properties in α-Fe will present not only a fundamental progress in defect physics but also a breakthrough to elucidate microscopic mechanism of hydrogen embrittlement in Fe-rich materials. Here we discuss possible implications of the hydrogen-enhanced vacancy activities (HEVA) in the hydrogen embrittlement phenomena.

The anisotropic vacancy clusterization induced by hydrogen can be directly linked with anisotropy observed in several fracture experiments. The {110} clusters are the first reasonable theoretical evidence of the enhancement of fracture along these slip planes of bcc metals experimentally observed.[41,42] Since $\langle 111\rangle$ are slip directions of bcc metals, the vacancy rows along these directions can be connected with the dislocation motions, which is also likely to contribute to fracture along the slip planes. On the other hand, the {100} tabular clusters directly lead to the void formation or crack nucleation on these cleavage planes of α-Fe. This is also consistent with fractures on these planes observed in some experiments.[42]

Moreover, the hydrogen-induced decrease of vacancy formation energy will be associated with the experimentally observed enhancement of dislocation mobility in the presence of hydrogen as the elastic shielding mechanism based on interstitial hydrogen.[12–14] Several dislocation motions such as cutting or jog climb-up are known to be accompanied by vacancy formations. In particular, the cutting motions are of great importance in a region with a high dislocation density, such as the region ahead of a crack tip. The formation energy decrease could be regarded as falloff of activation energies for such dislocation motions, so that it may contribute to increase of the dislocation mobility experimentally observed.[41,43]

In addition to the consistent explanations of experimental results, the HEVA has some advantages to the atomic-scale mechanism of hydrogen embrittlement in Fe-rich materials compared with the interstitial hydrogen effects dominantly discussed to date. As described in Sec. I, whether concentrations of interstitial hydrogen in highly stressed regions ahead of a crack tip are sufficient for the propagation has been still a long-standing issue in the endothermic materials. On the contrary, the vacancy-related processes provide a scenario that large (10^7 fold) increase of the concentration may occur without improbable accumulation of hydrogen.

Hydrogen-induced anisotropic vacancy clusters give a clear view to ''material thinning,'' an ambiguous concept used to date in the mechanisms with interstitial hydrogen. Compared to the preference of isotropic vacancy clusters in the case without hydrogen, the hydrogen trapping induces vacancy clusters with tabular shapes. This hydrogen effect on the shape of vacancy clusters can be closely related with hydrogen-enhanced generation of microcracks that are also planar voids.

We discuss the processes in the monovacancy formation and clusterization more intensively. For the former process, Frenkel-pair formations have considerably high activation energies.[44] Thus monovacancy formations accompanying with dislocation motions as well as near surface regions are more probable processes. Regarding the clusterization, coalescence of vacancies generated in distant regions is rather unlikely, since vacancy migration is suppressed by the hydrogen trapping.[45] In this respect, the relationship with dislocation motions that can directly introduce combined vacancy rows is of great importance for microcrack generation in highly deformed regions away from the surface.

Summarizing these results and considerations, HELP through HEVA is expected to be a promising mechanism for hydrogen embrittlement in Fe-rich materials. Owing to the relation with dislocation, the adsorption-induced dislocation emission[46] through HEVA might be also probable. In order to establish what microscopic effects are crucial, fair comparison between interstitial hydrogen and hydrogen-vacancy complex is still indispensable, which is now under study. Nevertheless, our present results strongly suggest that hydrogen-enhanced fracture through vacancy processes is expected to be more relevant to the microscopic mechanism of hydrogen embrittlement in Fe-rich materials.

IV. CONCLUSIONS

In conclusion, we have examined energetics of stability and clusterization of hydrogen-vacancy complexes in α-Fe, by means of *ab initio* supercell calculations. We have presented theoretical evidences of the hydrogen-enhanced vacancy formation in α-Fe, suggested in experiments. In particular, we have demonstrated a new stability of the hydrogen-monovacancy complexes, which corrects the conventional model frequently referred to date. Besides, we have predicted hydrogen-enhanced anisotropic vacancy clusterization based on our extensive calculations. These results are robust evidences for the relevance of vacancy-related processes to the atomic-scale mechanism of hydrogen embrittlement in Fe-rich materials, which have hardly been discussed as yet. Although further clarifications of hydrogen effects are still necessary, this point of view may be of great use for full understanding of the whole mechanism in those materials.

ACKNOWLEDGMENTS

We acknowledge Professor Y. Fukai and Professor M. Nagumo for their helpful discussions and suggestions. We also thank Dr. T. Miyazaki and Dr. Y. Morikawa for their help with the *ab initio* calculations. The calculations in this study have been performed on the Numerical Materials Simulator at NIMS.

---

[1] Y. Fukai and N. Okuma, Jpn. J. Appl. Phys., Part 2 **32**, L1256 (1993).

[2] M. Iwamoto and Y. Fukai, Mater. Trans., JIM **40**, 606 (1999).

[3] E. Hayashi, Y. Kurokawa, and Y. Fukai, Phys. Rev. Lett. **80**, 5588 (1998).

[4] Y. Fukai and N. Okuma, Phys. Rev. Lett. **73**, 1640 (1994).

[5] M. Nagumo, ISIJ Int. **41**, 590 (2001), and reference therein.

[6] M. Nagumo, M. Nakamura, and K. Takai, Metall. Mater. Trans. A **32A**, 339 (2001).

[7] M. Nagumo, K. Ohta, and H. Saitoh, Scr. Mater. **40**, 313 (1999).

[8] For a review, see S.M. Myers, M.I. Baskes, H.K. Birnbaum, J.W. Corbett, G.G. Deleo, S.K. Estreicher, E.E. Haller, N.M. Johnson, R. Kirchheim, S.J. Pearton, and M.J. Stavola, Rev. Mod. Phys. **64**, 559 (1992).

[9] A.R. Triano, Trans. Am. Soc. Met. **52**, 54 (1960).

[10] R.A. Oriani and R.H. Josephic, Acta Metall. **22**, 1065 (1974).

[11] C.D. Beachem, Metall. Trans. **3**, 437 (1972).

[12] H.K. Birnbaum and P. Sofronis, Mater. Sci. Eng., A **176**, 191 (1994).

[13] E. Sirois and H.K. Birnbaum, Acta Metall. Mater. **40**, 1377 (1992).

[14] P. Sofronis and H.K. Birnbaum, J. Mech. Phys. Solids **43**, 49 (1995).

[15] S.M. Myers, D.M. Follstaedt, F. Besenbacher, and J. Boettiger, J. Appl. Phys. **53**, 8734 (1982).

[16] F. Besenbacher, S.M. Myers, P. Nordlander, and J.K. Nörskov, J. Appl. Phys. **61**, 1788 (1987).

[17] P. Nordlander, J.K. Nörskov, F. Besenbacher, and S.M. Myers, Phys. Rev. B **40**, 1990 (1989).

[18] J.K. Nörskov, Phys. Rev. B **26**, 2875 (1982).

[19] Y. Fukai, *The Metal Hydrogen System* (Springer-Verlag, Berlin, 1993).

[20] S.M. Myers, P.M. Richards, W.R. Wampler, and F. Besenbacher, J. Nucl. Mater. **165**, 9 (1989).

[21] R.B. Mclellan and C.G. Harkins, Mater. Sci. Eng. **18**, 5 (1975).

[22] P. Ehrhart, P. Jung, H. Schultz, and H. Ullmaier, in *Atomic Defects in Metals*, edited by H. Ullmaier, Landolt-Börnstein, New Series, Group III, Vol. 25 (Springer-Verlag, Berlin, 1991).

[23] L. DeSchepper, D. Segers, L. Dorikens-Vanpraet, M. Dorikents, G. Knuyt, L.M. Stals, and P. Moser, Phys. Rev. B **27**, 5257 (1983).

[24] J.R. Beeler, Jr. and R.A. Johnson, Phys. Rev. **156**, 677 (1967).

[25] P. Hohenberg and W. Kohn, Phys. Rev. **136**, B804 (1964).

[26] W. Kohn and S.J. Sham, Phys. Rev. **140**, A1133 (1965).

[27] M.C. Payne, M.P. Teter, D.C. Allan, T.A. Arias, and J.D. Joannopoulos, Rev. Mod. Phys. **64**, 1045 (1992).

[28] Simulation Tool for Atom Technology (STATE), released by the Research Institute for Computational Sciences (RICS), National Institute of Advanced Industrial Science and Technology (AIST).

[29] D. Vanderbilt, Phys. Rev. B **40**, 7892 (1990).

[30] J.P. Perdew, J.A. Chevary, S.H. Vosko, K.A. Jackson, M.R. Pederson, D.J. Singh, and C. Fiolhais, Phys. Rev. B **46**, 6671 (1992).

[31] P. Bagno, O. Jepsen, and O. Gunnarsson, Phys. Rev. B **40**, 1997 (1989).

[32] P.A. Korzhavyi, I.A. Abrikosov, B. Johansson, A.V. Ruban, and H.L. Skriver, Phys. Rev. B **59**, 11 693 (1999).

[33] C. Kittel, *Introduction to Solid State Physics*, 6th ed. (Wiley, New York, 1987).

[34] E.G. Moroni, G. Kresse, J. Hafner, and J. Fürthmuller, Phys. Rev. B **56**, 15 629 (1997), and references therein.

[35] M.J. Gillan, J. Phys.: Condens. Matter **1**, 689 (1989).

[36] Y. Tateyama, T. Miyazaki, and T. Ohno (unpublished).

[37] The dissociation energy of H_2 in GGA calculations is shown to be inaccurate due to worse description of the H_2 molecule energy. Thus we use the experimental value for this quantity. See Ref. 30, and D.C. Patton, D.V. Porezag, and M.R. Pederson, Phys. Rev. B **55**, 7454 (1997).

[38] P. Söderlind, L.H. Yang, J.A. Moriarty, and J.M. Wills, Phys. Rev. B **61**, 2579 (2000).

[39] C. Domain and C.S. Becquart, Phys. Rev. B **65**, 024103 (2001).

[40] H. Sugimoto and Y. Fukai, Acta Metall. Mater. **40**, 2237 (1992).

[41] T. Tabata and H.K. Birnbaum, Scr. Metall. **18**, 231 (1984).

[42] A. Kimura and H. Kimura, Mater. Sci. Eng. **77**, 75 (1986).

[43] T. Tabata and H.K. Birnbaum, Scr. Metall. **17**, 947 (1983).

[44] H. J. Wollenberger, in *Physical Metallurgy*, edited by R. W. Cahn and P. Hassen, 3rd ed. (Elsevier, Amsterdam, 1983).

[45] Y. Tateyama and T. Ohno, ISIJ Int. **43**, 573 (2003).

[46] S.P. Lynch, Acta Metall. **20**, 2639 (1988).